



HAL
open science

Cross-Presentation of Skin-Targeted Recombinant Adenoassociated Virus 2/1 Transgene Induces Potent Resident Memory CD8⁺ T Cell Responses

David-Alexandre Gross, Alexandre Ghenassia, Laurent Bartolo, Dominique Urbain, Sofia Benkhelifa-Ziyyat, Stéphanie Lorain, Jean Davoust, Pascal Chappert

► **To cite this version:**

David-Alexandre Gross, Alexandre Ghenassia, Laurent Bartolo, Dominique Urbain, Sofia Benkhelifa-Ziyyat, et al.. Cross-Presentation of Skin-Targeted Recombinant Adenoassociated Virus 2/1 Transgene Induces Potent Resident Memory CD8⁺ T Cell Responses. *Journal of Virology*, 2019, 93 (5), pp.e01334-18. 10.1128/JVI.01334-18 . hal-03827009

HAL Id: hal-03827009

<https://hal.science/hal-03827009v1>


Submitted on 24 Oct 2022

HAL is a multi-disciplinary open access archive for the deposit and dissemination of scientific research documents, whether they are published or not. The documents may come from teaching and research institutions in France or abroad, or from public or private research centers.

L'archive ouverte pluridisciplinaire **HAL**, est destinée au dépôt et à la diffusion de documents scientifiques de niveau recherche, publiés ou non, émanant des établissements d'enseignement et de recherche français ou étrangers, des laboratoires publics ou privés.



Cross-Presentation of Skin-Targeted Recombinant Adeno-associated Virus 2/1 Transgene Induces Potent Resident Memory CD8⁺ T Cell Responses

David-Alexandre Gross,^a Alexandre Ghenassia,^{a*} Laurent Bartolo,^a Dominique Urbain,^a Sofia Benkhelifa-Ziyyat,^c Stéphanie Lorain,^c Jean Davoust,^a  Pascal Chappert^{a,b}

^aInstitut Necker Enfants Malades (INEM), INSERM U1151, CNRS UMR8253, Faculté de Médecine, Université Paris Descartes, Sorbonne Paris Cité, Paris, France

^bInovavion, Paris, France

^cMyology Research Center, UM76, INSERM U974, CNRS FRE 3617, Institut de Myologie, UPMC Université Paris 6, Sorbonne Universités, Paris, France

ABSTRACT A key aspect to consider for vaccinal protection is the induction of a local line of defense consisting of nonrecirculating tissue-resident memory T cells (T_{RM}), in parallel to the generation of systemic memory CD8⁺ T cell responses. The potential to induce T_{RM} has now been demonstrated for a number of pathogens and viral vectors. This potential, however, has never been tested for recombinant adeno-associated virus (rAAV) vectors, which are weakly inflammatory and poor transducer of dendritic cells. Using a model rAAV2/1-based vaccine, we determined that a single intradermal immunization with rAAV2/1 vectors in mice induces fully functional T_{RM} at the local site of immunization. The optimal differentiation of rAAV-induced transgene-specific skin T_{RM} was dependent on local transgene expression and additional CD4⁺ T cell help. Transgene expression in dendritic cells, however, appeared to be dispensable for the priming of transgene-specific skin T_{RM}, suggesting that this process solely depends on the cross-presentation of transgene products. Overall, this study provides needed information to properly assess rAAV vectors as T cell-inducing vaccine carriers.

IMPORTANCE rAAVs display numerous characteristics that could make them extremely attractive as vaccine carriers, including an excellent safety profile in humans and great flexibility regarding serotypes and choice of target tissue. Studies addressing the ability of rAAV to induce protective T cell responses, however, are scarce. Notably, the potential to induce a tissue-resident memory T cell response has never been described for rAAV vectors, strongly limiting further interest for their use as vaccine carriers. Using a model rAAV2/1 vaccine delivered to the skin, our study demonstrated that rAAV vectors can induce bona fide skin resident T_{RM} and provides additional clues regarding the cellular mechanisms underlying this process. These results will help widen the field of rAAV applications.

KEYWORDS cross-presentation, rAAV vaccine, resident memory T cells, skin

Tissue-resident memory T cells (T_{RM}) are an essential component of the T cell arm of the adaptive immune memory response toward a large variety of pathogens (1, 2). T_{RM} can be found in almost all tissues in challenged laboratory mice (3, 4) and in humans (5, 6), where they naturally serve as sentinels poised to continuously scan the local tissue for their cognate antigen and rapidly clear infected cells (7). Additionally, by rapidly secreting proinflammatory cytokines such as gamma interferon (IFN-γ), tumor necrosis factor alpha (TNF-α), or interleukin 2 (IL-2) upon activation, T_{RM} also play a central role in the orchestration of local secondary immune responses by recruiting and activating various other actors of innate and adaptive immunity (2, 8, 9).

Citation Gross D-A, Ghenassia A, Bartolo L, Urbain D, Benkhelifa-Ziyyat S, Lorain S, Davoust J, Chappert P. 2019. Cross-presentation of skin-targeted recombinant adeno-associated virus 2/1 transgene induces potent resident memory CD8⁺ T cell responses. *J Virol* 93:e01334-18. <https://doi.org/10.1128/JVI.01334-18>.

Editor Rozanne M. Sandri-Goldin, University of California, Irvine

Copyright © 2019 American Society for Microbiology. All Rights Reserved.

Address correspondence to David-Alexandre Gross, david.gross@inserm.fr, or Pascal Chappert, pascal.chappert@inserm.fr.

* Present address: Alexandre Ghenassia, Centre de Recherches en Cancérologie de Toulouse (CRCT), INSERM U1037, Toulouse, France.

Received 3 August 2018

Accepted 3 December 2018

Accepted manuscript posted online 12 December 2018

Published 19 February 2019

T_{RM} have been shown to differentiate *in situ* from $KLRG1^-$ memory precursors under the control of tissue-derived signals, such as IL-15 or transforming growth factor β (TGF- β) in the skin (10, 11). The role of local antigen recognition for the development and maintenance of T_{RM} , however, seems to differ between tissues (12). In the skin, T_{RM} do not rely on secondary T cell receptor (TCR) signaling events for differentiation and maintenance (13, 14). Yet antigen-specific skin T_{RM} formation is significantly enhanced in the presence of cognate antigen (15, 16). The exact nature of the antigen-presenting cells involved in both the initial priming and an eventual secondary encounter in the local microenvironment is still unclear and likely differs depending on the nature of the pathogen and the tissue. A key role for antigen cross-presentation by DNGR1⁺ dendritic cells (DCs) has nonetheless been shown in the context of vaccinia and influenza virus infection (17).

In mice, the induction of T_{RM} in the skin or other nonlymphoid tissues (NLT) has now been documented following several local viral infections or viral vector immunizations, including herpes simplex virus (HSV) (18, 19), lymphocytic choriomeningitis virus (LCMV) (3, 20), murine cytomegalovirus (MCMV) (21, 22), vaccinia virus (VACV) (15, 23), vesicular stomatitis virus (VSV) (24, 25), influenza virus (26), and West Nile virus (27) as well as the nonreplicating modified vaccinia Ankara (MVA) strain of VACV (16), human papillomavirus vectors (HPV pseudoviruses) (28), and adenovirus vectors (29). Such potential, however, has never been reported for recombinant adeno-associated virus (rAAV) vectors. rAAVs are nonreplicative but can lead to high levels of transgene expression in the target tissue. rAAVs further display numerous serotypes and capsid variants and present a good safety profile in humans, making them attractive vaccine carriers (30). rAAVs, however, are weakly inflammatory and poor transducers of DCs (31–33), two unique properties that are not shared with most vectors commonly used to study T_{RM} induction.

We report here that a single intradermal immunization with a model rAAV2/1 vector was sufficient to induce potent T_{RM} at the local site of immunization. We additionally demonstrate that local transgene expression and CD4⁺ T cell help are key for the optimal priming of transgene-specific skin T_{RM} following rAAV immunization, while transgene expression in DCs is not required.

RESULTS

Intradermal immunization with rAAV2/1 vector induces transgene-specific skin resident memory CD8⁺ T cells. We have previously described in detail the generation of systemic anti-transgene effector (T_{EM}) and central memory (T_{CM}) CD8⁺ T cells following both intramuscular and intradermal immunization with an rAAV2/1 vector (34). To further investigate whether intradermal immunization also gave rise to tissue resident memory CD8⁺ T cell responses at the site of immunization, we used the same rAAV2/1 vector, which encodes a full-length membrane-bound form of the ovalbumin model antigen fused to the UTY₂₄₆ and DBY₆₀₈ male HY antigen epitopes (rAAV2/1-mOVA-HY). Intramuscular and intradermal immunization with such an rAAV2/1 construct induces strong OVA₂₅₇-specific CD8⁺ T cell responses in female mice in the presence of a concomitant DBY₆₀₈-specific CD4⁺ T cell response.

As previously published (34), no significant differences could be seen in the frequencies of OVA₂₅₇-specific CD8⁺ T cells in the peripheral blood of intramuscularly and intradermally immunized female mice up to 60 days postimmunization (Fig. 1A). Interestingly, a significant OVA₂₅₇-specific CD8⁺ T cell population could still be detected in both the dermis and epidermis of intradermally, but not intramuscularly, immunized female mice by day 60 (Fig. 1B and C), at a time when transgene expression is undetectable (34). On average, around 10⁴ OVA₂₅₇⁺ CD8⁺ T cells could be recovered per injected ear, representing a 300-fold increase in OVA₂₅₇⁺ CD8⁺ T cell numbers compared to ears of mice injected intramuscularly or to control vector-injected ears. Importantly, epidermal resident OVA₂₅₇⁺ memory CD8⁺ T cells harbored a classical CD69⁺ CD103⁺ $KLRG1^-$ CD44^{hi} CD127^{low/neg} CD62L⁻ Ki-67^{low} resting tissue resident memory T cell phenotype (Fig. 1D to F). Dermal resident OVA₂₅₇⁺ memory CD8⁺ T cells

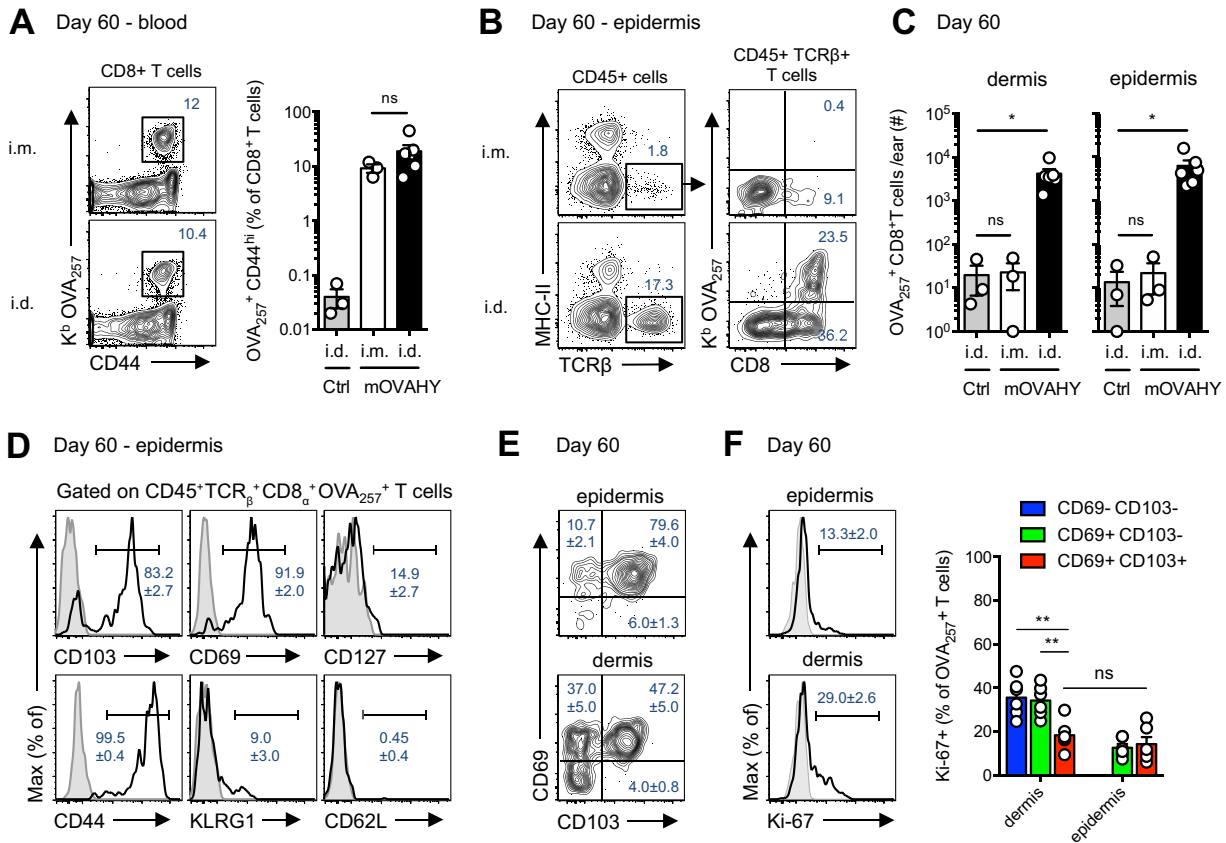


FIG 1 Intradermal immunization with rAAV2/1 vector induces transgene-specific skin CD8⁺ T_{RM}. Skin resident anti-OVA memory CD8⁺ T cells were analyzed between day 60 and day 70 after immunization in the ears of female mice immunized in the tibialis anterior (i.m.) or ear dermis (i.d.) with rAAV2/1-mOVA-HY (mOVA-HY) or a control rAAV2/1 vector (Ctrl). (A) Representative dot plots for CD44 and K^b/OVA₂₅₇ tetramer staining (left) and frequencies of OVA₂₅₇⁺ CD44^{hi} cells in live blood CD8⁺ T cells (right). (B) Representative dot plots for MHC-II and TCRβ staining in live epidermal MHC-II⁻ TCRβ⁺ T cells (right) from a female mouse immunized i.m. (top) or i.d. (bottom) with the mOVA-HY construct. (C) Absolute numbers of live CD45⁺ MHC-II⁻ TCRβ⁺ OVA₂₅₇⁺ CD8⁺ T cells recovered from the dermis or epidermis of indicated mice. Values are means ± SEM (*n* = 3 Ctrl i.d., *n* = 3 mOVAHY i.m., and *n* = 6 mOVAHY i.d. mice per group, pooled from 2 independent experiments). ns, not significant. *, *P* < 0.05 (Mann-Whitney test). (D and E) Representative histograms for CD103, CD69, CD127, CD44, KLRG1, and CD62L expression (black unfilled), compared to an unstained control (gray filled) (D), and representative dot plots for CD103 and CD69 (E) staining in live CD45⁺ MHC-II⁻ TCRβ⁺ OVA₂₅₇⁺ CD8⁺ T cells isolated from the dermis or epidermis of female mice immunized i.d. with the mOVA-HY construct. Average frequencies of expressing cells for each individual marker are displayed as means ± SEM (*n* = 6 mice for CD103, CD69, and CD44 and *n* = 3 mice for all other markers). (F) Representative histograms for Ki-67 expression (black unfilled) (left), compared to an unstained control (gray filled), and average frequencies of Ki-67-expressing cells in skin resident OVA₂₅₇⁺ subpopulations isolated from the dermis or epidermis of female mice immunized i.d. with the mOVA-HY construct. Values are means ± SEM (*n* = 6 pools of 3 mice each, pooled from two independent experiments). **, *P* < 0.01 (repeated measures one-way analysis of variance [ANOVA], Bonferroni's test).

also consisted of a majority of CD69⁺ CD103⁺ OVA₂₅₇⁺ CD8⁺ T cells (47.2% ± 5.0%), albeit mixed with higher frequencies of CD69⁺ CD103⁻ cells (37.0% ± 5.0%) (Fig. 1E). A small CD69⁻ CD103⁻ OVA₂₅₇⁺ CD8⁺ T cell subset (11.7% ± 1.8%), putatively circulating effector/memory CD8⁺ T cells, could also be detected in the dermis. Both CD69⁺ CD103⁻ and CD69⁻ CD103⁻ subpopulations expressed slightly higher levels of Ki-67 (Fig. 1F), suggesting that they might contain more recently activated cells.

Local transgene expression drives transgene-specific skin CD8⁺ T_{RM} differentiation. Recent studies suggest that local antigen expression acts as a key determinant of T_{RM} differentiation *in vivo* (15, 16). To assess the role of local transgene expression in the differentiation of rAAV-induced T_{RM}, we immunized female mice simultaneously in one ear with an OVA-expressing rAAV2/1 vector and in the opposite ear with a control rAAV2/1 vector (rAAV2/1-Ctrl) (Fig. 2A). In line with the limited intrinsic inflammatory potential of rAAV vectors, no external sign of inflammation could be observed in the rAAV2/1-Ctrl injected ear [mOVAHY (distal)] throughout the course of the ongoing systemic anti-OVA immune response. In contrast, a clear swelling of the

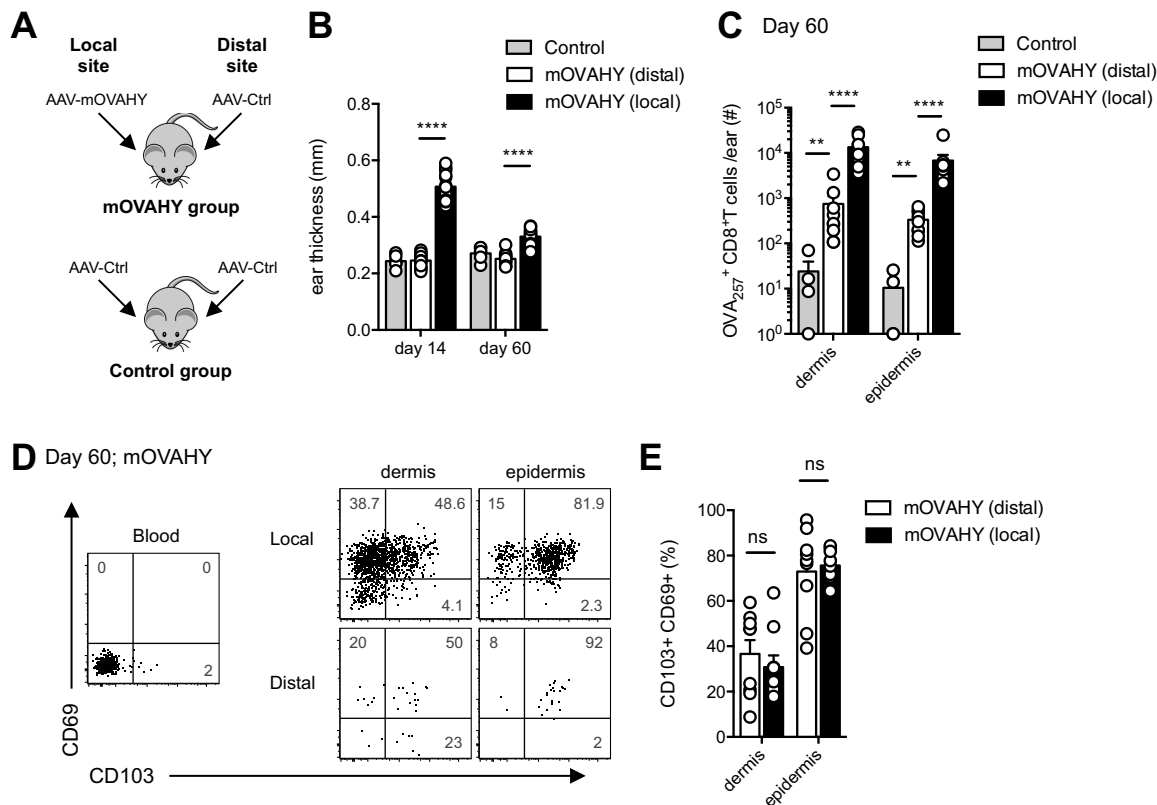


FIG 2 Local transgene expression drives transgene-specific skin CD8⁺ T_{RM} differentiation. (A) Female mice were immunized in one ear dermis with rAAV2/1-mOVA-HY (local site) and in the opposite ear dermis (distal site) with a control rAAV1 vector. As control, a second set of female mice was immunized in the dermis of both ears with the control rAAV2/1 vector. (B) Ear thickness was measured at the indicated time points after immunization. Values are means ± SEM ($n = 6$ control and 13 mOVAHY [local/distal] samples per group and per time point pooled from 2 independent experiments). ****, $P < 0.0001$ (two-way ANOVA/Sidak's test). (C) Skin resident anti-OVA memory CD8⁺ T cells were analyzed at day 60 after immunization in indicated ears. The graph shows the absolute numbers of live CD45⁺ MHC-II⁻ TCRβ⁺ OVA₂₅₇⁺ CD8_α⁺ T cells recovered from the dermis or epidermis of mice. (D) Representative dot plots for CD103 and CD69 staining and (E) frequencies of CD69⁺CD103⁺ cells in live CD45⁺ MHC-II⁻ TCRβ⁺ OVA₂₅₇⁺ CD8_α⁺ T cells from blood and dermis or epidermis cell suspensions of ears of immunized female mice. Values are means ± SEM ($n = 4$ control and 9 mOVAHY [local/distal] samples, pooled from 3 independent experiments). **, $P < 0.01$; ****, $P < 0.0001$ (Mann-Whitney test).

rAAV2/1-mOVAHY injected ear [mOVAHY (local)] could be seen by day 14 (Fig. 2B), corresponding to the peak of the primary T cell response. Minor residual swelling was also detected up to day 60.

Mirroring the enhanced swelling, local mOVAHY transgene expression clearly dictated the recruitment of OVA₂₅₇-specific skin resident CD8⁺ T cells (Fig. 2C). On average, 33.2 ± 5.5 and 22.6 ± 4.9 times more OVA₂₅₇⁺ CD8⁺ T cells could be detected by day 60 in the dermis and epidermis, respectively, of the mOVAHY-immunized ear [mOVAHY (local)] than in the contralateral ear [mOVAHY (distal)]. It should further be noted that the contralateral rAAV2/1-Ctrl-immunized ears of rAAV2/1-mOVAHY-immunized mice did harbor a sizeable population of OVA₂₅₇⁺ CD8⁺ T cells, ranging from 3×10^2 to 2×10^3 cells per ear (Fig. 2C). A vast majority of them expressed CD69 and CD103 (Fig. 2D and E), two markers not expressed on blood-circulating OVA₂₅₇⁺ memory CD8⁺ T cells. It is thus unlikely that these cells simply reflect bystander contamination from blood-circulating effector/memory T cells.

Overall, these results confirm a key role for local antigen expression in the recruitment of transgene-specific T_{RM}. They also highlight distal seeding of a small population of bona fide transgene-specific T_{RM} independently of local antigen expression or strong local inflammatory signals.

Intradermal immunization with rAAV2/1 vector induces functional skin CD8⁺ T_{RM}. T_{RM}-mediated protection against secondary viral challenges relies in part on direct

lytic activity against infected cells. Additionally, the capacity of T_{RM} to rapidly secrete proinflammatory cytokines, most notably IFN- γ , is essential to activate and recruit other immune cells at the site of infection (2).

First, we tested the cytokine secretion potential of rAAV-induced CD8⁺ T_{RM}. Sixty days after intradermal immunization with rAAV2/1-mOVAHY, most isolated dermal and epidermal OVA₂₅₇-responsive CD8⁺ T cells were capable of secreting both IFN- γ and TNF- α upon *in vitro* restimulation with their cognate peptide (Fig. 3A). Among those, around 10% additionally exhibited IL-2 secretion potential. The polyfunctional profile of rAAV2/1-induced T_{RM} thus appeared similar to, if not enhanced above, that of draining lymph node (LN) or splenic resident effector/memory OVA₂₅₇⁺ CD8⁺ T cells (Fig. 3B). To test whether this cytokine secretion potential translated *in vivo* into rapid recruitment of immune partners at the site of immunization, female mice were coimmunized with rAAV2/1-mOVAHY (local site) and rAAV2/1-Ctrl vectors (distal site) and 60 days later were challenged in both ears with either OVA₂₅₇ or SMCY₇₃₈ control peptide. Strong swelling could readily be detected 20 h after OVA₂₅₇ peptide challenge in the mOVAHY-immunized ear (local/OVA₂₅₇) (Fig. 3C). Swelling was maximal 44 h postchallenge and was associated with increased recruitment of CD45⁺ hematopoietic cells (Fig. 3D), including inflammatory monocytes and neutrophils. Interestingly, OVA₂₅₇ peptide challenge in the contralateral ear (distal/OVA₂₅₇) led to reduced yet significant swelling (Fig. 3C). Notably, a small, albeit significant, recruitment of inflammatory monocytes could be detected (Fig. 3D). This suggests that even a few hundreds OVA₂₅₇⁺ T_{RM}, as detected at this distal site (Fig. 2C), could have a biological antigen-specific impact on secondary immune responses. Of note, slight swelling could also be observed early following SMCY₇₃₈ peptide challenge in mOVAHY-immunized ears (local/SMCY₇₃₈). This could reflect an additional noncognate activation of T_{RM} with local biological consequences in the presence of high numbers of T_{RM}.

Second, we tested the cytotoxic potential of rAAV2/1-induced skin OVA₂₅₇⁺ T_{RM}. Sixty days after intradermal immunization with rAAV2/1-mOVAHY, a majority of isolated splenic, lymph node resident, dermal, and epidermal OVA₂₅₇-responsive IFN- γ ⁺ CD8⁺ T cells were capable of mobilizing CD107 at the plasma membrane, a marker of active degranulation, upon *in vitro* restimulation with cognate peptide (Fig. 3E and F). These cells additionally expressed granzyme B (Fig. 3F). It can be noted that epidermal OVA₂₅₇⁺ T_{RM} showed a lower CD107 mobilization potential than dermal or secondary lymphoid organ resident OVA₂₅₇⁺ (Fig. 3F). This, however, is in line with a recent observation in human lung resident CD69⁺ CD103⁺ CD8⁺ T_{RM} (35). To further assess how this translated *in vivo*, female mice were immunized in the ear with an rAAV2/1-mOVAHY or control (Ctrl) vector and 70 days later were challenged with a secondary intradermal injection of rAAV2/8-sOVA vector. To control for a potential impact of circulating effector/memory OVA₂₅₇⁺ CD8⁺ T cells, mice were continuously treated, starting 1 day prior to the secondary challenge, with an S1P receptor agonist, FTY720, to block T cell egress from lymph nodes. A group of intramuscularly immunized mice, which harbor similar frequencies of systemic—but not skin resident—OVA₂₅₇⁺ memory T cells (Fig. 1A), was also included in the experiment. Eight days later, an enhanced IFN- γ response (Fig. 3G) and 10-fold-lower level of OVA mRNA expression (Fig. 3H) were detected in mice preimmunized intradermally with the rAAV2/1-mOVAHY vector compared to those in intramuscularly immunized mice. This result confirms the potential of locally induced transgene-specific T_{RM} to reactivate in the context of a secondary challenge and to participate in the killing of infected cells. The FTY720 treatment used in these experiments, however, did not fully prevent circulating memory CD8⁺ T cell egress from participating to the local immune response, as seen in intramuscularly immunized mice (Fig. 3G and H). This unfortunately prevented us from properly assessing the cytotoxic potential of the low frequency of transgene-specific T_{RM} seeding distal skin sites.

Overall, these experiments nonetheless demonstrate that rAAV vector can induce the differentiation of fully functional transgene-specific skin T_{RM} at the site of immunization.

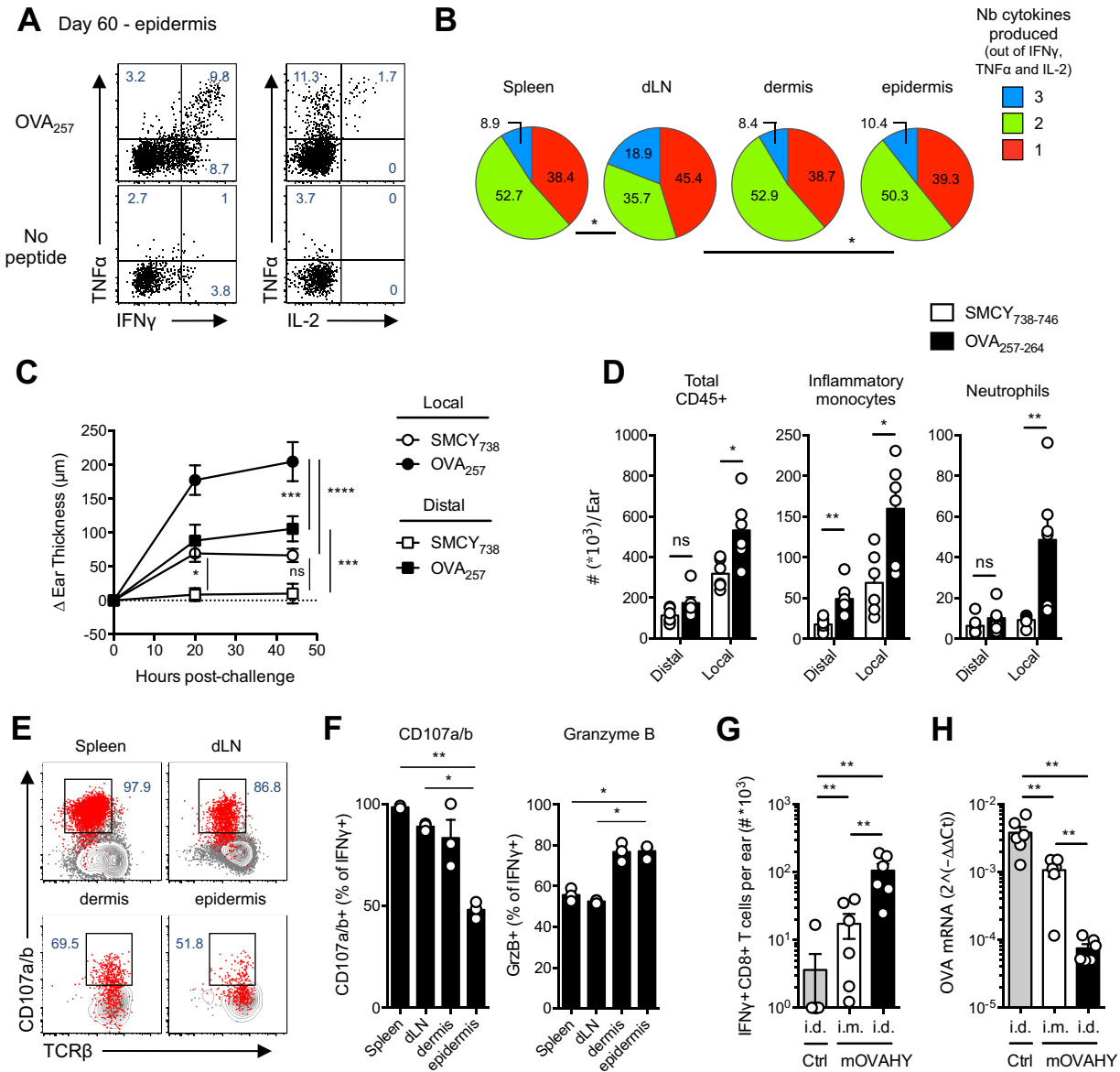


FIG 3 Intradermal immunization with rAAV2/1 vector induces functional skin CD8⁺ T_{H1} cells. (A and B) Female mice were immunized in the ear dermis with rAAV2/1-mOVA-HY (mOVA-HY). At day 60, draining lymph node or epidermal or dermal cell suspensions, pooled from 3 individual mice for each sample, were restimulated *in vitro* with OVA₂₅₇ peptide (1 μg/ml) and subsequently stained for IFN- γ , TNF- α , and IL-2 production. (A) Representative dot plots for IFN- γ and TNF- α (left) or TNF- α and IL-2 (right) expression in OVA₂₅₇-stimulated (top) or unstimulated (bottom) live epidermal CD45⁺ MHC-II⁻ TCR β ⁺ CD8⁺ T cells. (B) Relative proportion of single (red)-, double (green)-, and triple (blue)-cytokine-producing OVA₂₅₇-stimulated live CD8⁺ T cells from the indicated organs ($n = 4$ pools of 3 mice each, pooled from 2 independent experiments). Analysis and presentation of distributions were performed using SPICE version 5.35 on background (unstimulated) corrected data. Comparison of distributions was performed using a Student t test and a partial permutation test as previously described (53). *, $P < 0.05$. (C to E) Female mice were immunized in one ear dermis with rAAV2/1-mOVA-HY (local) and in the opposite ear dermis (distal) with a control rAAV2/1 vector. At day 60, mice were challenged in both ears with either OVA₂₅₇ or unrelated SMCY peptide. (C) Ear swelling at the indicated time point postchallenge. (D) Absolute number of live CD45⁺ cells (left), CD45⁺ CD11b⁺ Ly6C^{hi} Ly6G⁻ inflammatory monocytes (middle), and CD45⁺ CD11b⁺ Ly6C^{int} Ly6G⁺ neutrophils (right) in the ears of mice. Values are means \pm SEM ($n = 6$ mice/group, pooled from 2 independent experiments). *, $P < 0.05$; **, $P < 0.01$; ***, $P < 0.001$; ****, $P < 0.0001$ (2-way ANOVA/Sidak test [C] and Mann-Whitney test [D]). (E and F) Female mice were immunized in the ear dermis with rAAV2/1-mOVA-HY. At day 60, draining lymph node or epidermal or dermal cell suspensions, pooled from 3 individual mice, were restimulated *in vitro* with OVA₂₅₇ peptide (1 μg/ml) in the presence of anti-CD107 a and CD107b antibodies (CD107a/b) and subsequently stained for IFN- γ and granzyme B (GrzB) production. Shown are representative dot plots for CD107a/b and TCR β expression in IFN- γ ⁺ OVA₂₅₇-stimulated (red) or total unstimulated (gray) (E) and background (unstimulated group)-corrected frequencies of CD107a/b⁺ (left) and GrzB⁺ (right) cells among live CD45⁺ MHC-II⁻ CD8⁺ T cells from indicated organs (F). Values are means \pm SEM ($n = 3$ pools of 3 mice each). *, $P < 0.05$; **, $P < 0.01$ (RM one-way ANOVA, Bonferroni's test). (G and H) Female mice were immunized i.m. or i.d. with rAAV2/1-mOVA-HY (mOVA-HY) or a control rAAV2/1 vector (Ctrl). At day 70, all mice were challenged in the ear dermis with rAAV2/8-sOVA and maintained under FTY720 treatment until the end of the experiment. (G) Absolute numbers of live CD44^{hi} IFN- γ ⁺ CD8⁺ T cells following *in vitro* restimulation with OVA₂₅₇ peptide (1 μg/ml); (H) OVA mRNA expression in challenged ear 8 days later. Values are means \pm SEM ($n = 6$ mice/group, pooled from 2 independent experiments). **, $P < 0.01$ (Mann-Whitney test).

Cross-presentation of skin-targeted rAAV transgene is sufficient to induce transgene-specific skin resident memory CD8⁺ T cells. All experiments described so far were performed in female mice. The strong anti-transgene DBY₆₀₈-specific CD4⁺ T cell response that can be seen in female hosts significantly boosts systemic anti-transgene CD8⁺ T cell responses following rAAV2/1 intradermal immunization (34). Additionally, previous studies have clearly shown that pseudotyped rAAV vector are not all equal regarding dendritic cell transduction. And this parameter can influence the resulting direct priming of anti-transgene CD8⁺ T cell responses (32, 33, 36). We thus tested the impact of both parameters, antigen expression in DCs and CD4⁺ T cell help, on T_{RM} formation upon rAAV2/1-mediated intradermal immunization.

The addition of four repeats of the miR142-3p target sequence downstream of the mOVAHY transgene inhibits its expression in DCs (34), in line with the prevalent miR142-3p expression found in all hematopoietic cells (37). Interestingly, similar numbers of skin resident OVA₂₅₇⁺ CD8⁺ T cells could be recovered from immunized female mice with both wild-type (WT) (mOVAHY) and miR142-3p-regulated constructs (mOVAHY-miR) (Fig. 4A). The phenotype (Fig. 4B and C) and polyfunctionality (Fig. 4D) of OVA-specific T_{RM} induced by both constructs further appeared indistinguishable. This demonstrates that in the presence of CD4⁺ T cell help, cross-presentation events initiated after rAAV vector transduction of nonhematopoietic skin cells are sufficient to induce the accumulation of bona fide T_{RM} in the skin.

To further test for the role of CD4 T cell help, we used the fact that male mice are naturally tolerant to male antigens and do not mount a DBY₆₀₈-specific CD4⁺ T cell response, as evidenced previously (34). Accordingly, anti-transgene CD8⁺ T cell responses tracked in male mice in response to rAAV2/1-mOVAHY immunization fully mimic the responses seen in CD4-depleted female mice (38). Following intradermal immunization, the absence of CD4⁺ T cell help did lead to a clear reduction in the number of recovered skin resident OVA₂₅₇⁺ CD8⁺ T cells (Fig. 4E). This reduction, however, appears to fully correlate with the reduced frequency of systemic CD8⁺ T cells seen in the peripheral blood (Fig. 4E). Furthermore, the absence of CD4⁺ T cell help did not seem to reproducibly impact the repartition of OVA-specific CD8⁺ T_{RM} between the dermal and the epidermal layers of the skin as well as their expression of CD69 and CD103 (Fig. 4E). These results thus suggest that CD4⁺ T cell help mostly regulates the overall strength of the anti-transgene immune response rather than having a direct influence on skin T_{RM} differentiation.

Finally, we tested for a possible synergy between cross-presentation and CD4⁺ T cell help, as previously seen following intramuscular immunization (34). In line with our observations in female mice, however, circulating and skin resident OVA-specific CD8⁺ T cell responses against both WT and miR142-3p-regulated constructs appeared to be similar in male mice (Fig. 4F). This further extends our previous observation that transgene expression in hematopoietic cells is dispensable for the full induction of systemic T cell responses in the context of skin targeting with rAAV vectors (34).

DISCUSSION

Targeting the skin allows for the induction of a local line of defense in the form of tissue-resident memory CD8⁺ T cells (1, 2, 23), a result that we reproduced in this study in the context of a model rAAV2/1-based vaccine. Of interest, our study additionally suggested that *in situ* differentiation of rAAV-induced transgene-specific skin CD8⁺ T_{RM} follows the same rules—with respect to antigen presentation, CD4⁺ T cell help, or local antigen—as have previously been described in the context of more inflammatory viral vectors.

While T_{RM} have been described in many infectious or vaccine models, the impact of the viral vector itself on the induction of CD8⁺ T_{RM} has not yet been clearly addressed. Among known differences between rAAV vectors and other viral vectors, a key characteristic is their low inflammatory potential (39, 40). rAAVs are also nonreplicating, and transgene expression in target tissue is usually only maximal by 2 to 3 weeks (41, 42). This leads to delayed anti-transgene immune response with initial T cell priming only

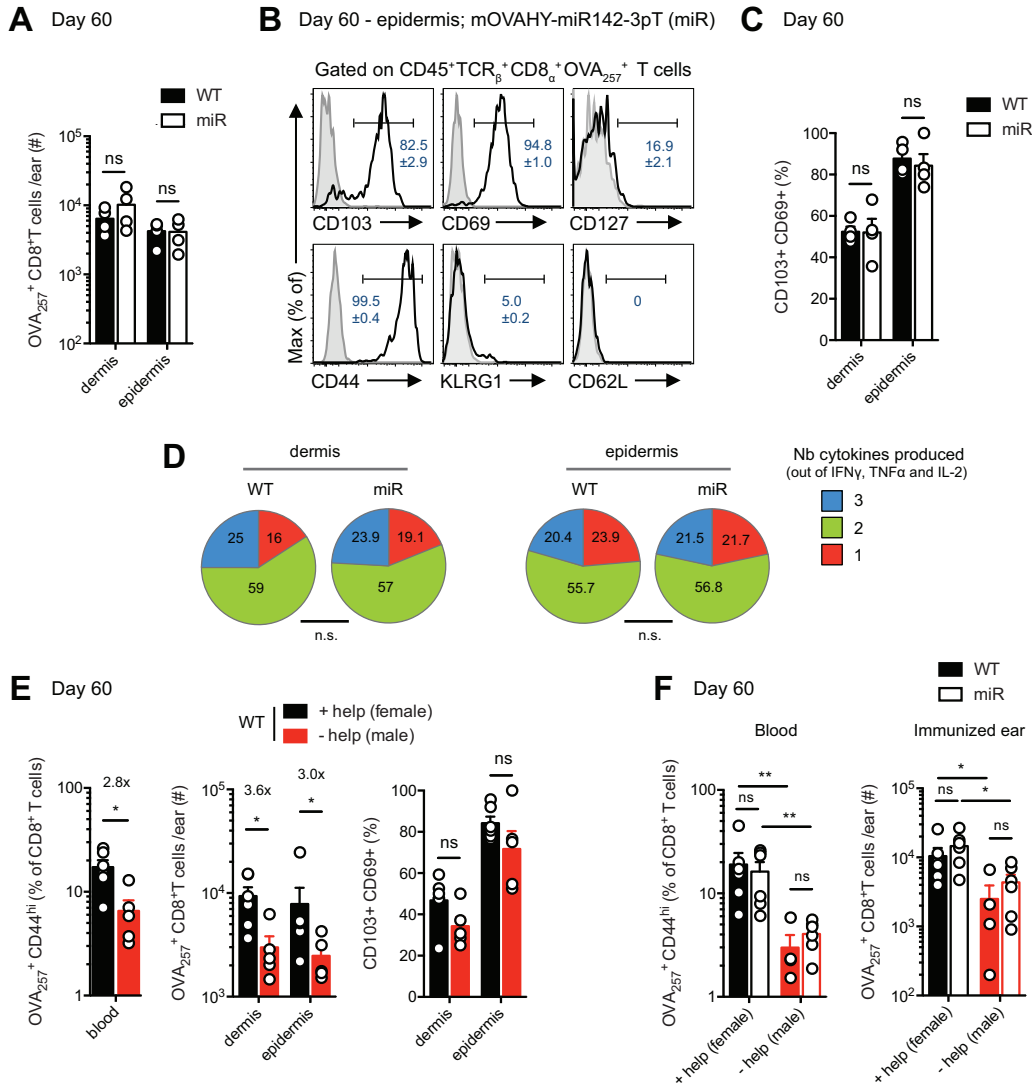


FIG 4 Cross-presentation of skin-targeted rAAV transgene, in the presence of CD4⁺ T cell help, is sufficient to induce transgene-specific skin resident memory CD8⁺ T cells. (A to D) Female mice were immunized in the ear dermis with rAAV2/1-mOVA-HY (WT) or rAAV2/1-mOVA-HY-miR142-3pT (miR). Skin resident anti-OVA memory CD8⁺ T cells were analyzed at day 60 after immunization in the indicated ears. (A to C) Absolute numbers of live CD45⁺ MHC-II⁻ TCRβ⁺ OVA₂₅₇⁺ CD8_α⁺ T cells (A), representative histograms for CD103, CD69, CD127, CD44, KLRG1, and CD62L expression (B), and frequencies of CD69⁺ CD103⁺ cells in live epidermal CD45⁺ MHC-II⁻ TCRβ⁺ OVA₂₅₇⁺ CD8_α⁺ T cells in the dermis or epidermis of immunized ears (C). In panel B, frequencies of expressing cells for each individual marker are displayed as means ± SEM and compared to an unstained control (gray). Mean ± SEM (*n* = 4 mice per group). (D) Relative proportions of single (red)-, double (green)-, and triple (blue)-cytokine-producing OVA₂₅₇ stimulated live CD8_α⁺ T cells from indicated immunized dermis or epidermis following *in vitro* restimulation with OVA₂₅₇ peptide (1 μg/ml). Analysis was performed as described for Fig. 3B. (E) Female or male mice were immunized in the ear dermis with rAAV2/1-mOVA-HY (WT). Shown are frequencies of OVA₂₅₇⁺ CD44^{hi} cells in live CD8⁺ T cells in the blood (left), absolute numbers of live CD45⁺ MHC-II⁻ TCRβ⁺ OVA₂₅₇⁺ CD8_α⁺ T cells (middle), and frequencies of CD69⁺ CD103⁺ cells in live CD45⁺ MHC-II⁻ TCRβ⁺ OVA₂₅₇⁺ CD8_α⁺ T cells (right) in the dermis or epidermis of immunized ears at day 60 postimmunization. Average fold changes between male and female mice are additionally displayed above the bars corresponding to each tissue. Values are means ± SEM (*n* = 5/6 mice per group pooled from 2 independent experiments). *, *P* < 0.05 (Mann-Whitney test). (F) Female or male mice were immunized in the ear dermis with rAAV2/1-mOVA-HY (WT) or rAAV2/1-mOVA-HY-miR142-3pT (miR). Shown are frequencies of OVA₂₅₇⁺ CD44^{hi} cells among live CD8⁺ T cells in the blood (left) and absolute numbers of live CD45⁺ MHC-II⁻ TCRβ⁺ OVA₂₅₇⁺ CD8_α⁺ T cells in immunized ears (right) at day 60 postimmunization. Values are means ± SEM (*n* = 4/6 mice per group pooled from 3 independent experiments). *, *P* < 0.05; **, *P* < 0.01 (Mann-Whitney test).

seen by day 5 in the draining lymph nodes (dLNs) (34) and a peak of OVA₂₅₇⁺ CD8⁺ T cells in the spleen, blood, and tissue by day 14 (reference 34 and unpublished observations). Nonreplicating viral vectors have already been used to induce T_{RM} in the skin (16) or vaginal mucosa (28, 29), although lower numbers of T_{RM} were reported

following immunization with MVA than with replicating VACV in the skin (16). In our hands, the average number of OVA₂₅₇⁺ memory CD8⁺ T cells that could be recovered per injected ear at the late memory stage of the response matched the numbers of T_{RM} previously reported for the ear at similar time points following VACV infection (16). Most importantly, OVA₂₅₇⁺ memory CD8⁺ T_{RM} recovered at the site of injection appeared to be fully functional, both at clearing cells infected in the context of a secondary challenge and at recruiting other components of the immune system. Comparisons with other studies on skin T_{RM}, however, are hindered by differential choices of target skin sites. Most studies target the flank skin. In contrast, the mouse ear, like most human skin, is devoid of panniculus carnosus. It thus represents a better site for rAAV intradermal immunization, avoiding potential interferences from bystander rAAV transduction of underlying smooth muscle cells (43, 44).

Another key question that we addressed in this study is whether induction of said T_{RM} follows rules in the context of rAAV immunization similar to those previously observed for other viruses. Our unique model allowed us to address three parameters of the immune response previously linked to T_{RM} induction: CD4⁺ T cell help, cross-priming, and local antigen expression. Local antigen has been previously described to boost T_{RM} differentiation in the skin in the context of MVA (16), VACV (15), and HSV (45) immunization. Following similar principles, rAAV2/1-induced T_{RM} formation appeared to be maximal at the site of immunization, while only a small number of transgene-specific T_{RM} could be seen at a distal site receiving irrelevant rAAV2/1 immunization. It remains to be seen whether multiple immunizations would enhance such distal T_{RM} formation and favor the induction of broad protection, as previously suggested (23, 45).

A key particularity of rAAV vectors is their limited transduction of professional antigen-presenting cells (32, 33, 36). We have previously shown that following intradermal immunization with rAAV2/1 vectors, transgene-derived peptides are cross-presented both by resident CD8 α ⁺ and migratory CD103⁺ and CD11b⁺ DCs (34). The source of antigen, however, differs. Resident CD8 α ⁺ DCs mostly process antigens from transduced hematopoietic cells, while migratory DCs also present antigens from transduced nonhematopoietic skin cells. Importantly, these cross-presentation events are sufficient for the full induction of systemic memory cytotoxic T lymphocyte (CTL) responses. Our current study now extends this observation to the induction of skin CD8⁺ T_{RM}. A previous study in the context of vaccinia virus infection in the skin nicely showed that cross-presentation by DNRG1⁺ DCs, regrouping both resident CD8 α ⁺ and migratory CD103⁺ DCs, was required for the full induction of skin CD8⁺ T_{RM}. We now demonstrate that inhibiting transgene expression in hematopoietic cells does not impair anti-transgene skin CD8⁺ T_{RM} formation. This result suggests that the sole cross-presentation of tissue-expressed viral antigen/transgene is not only required but also sufficient for the induction of skin CD8⁺ T_{RM}. This property is of particular interest for pseudotyped rAAV vectors with even lower capacities for DC transduction than the rAAV2/1 vector used in this study (32, 33, 36). The logical follow-up question then becomes which cell(s) in the skin needs to be transduced by the rAAV vector to drive optimal local and systemic immunity. While no definite answer exists for this question so far, it can be noted that the potential to transduce keratinocytes has been described for some rAAV serotypes (44, 46, 47). However, it appears quite limited (48). More recently, transgene expression in the sensory neurons of the trigeminal ganglia has also been reported following intradermal immunization with various rAAV serotypes in the whiskerpad in mice (49), of which the rAAV2/1 serotype used in our study achieved the highest level of gene expression.

The last point that we addressed in this study concerns the specific role of CD4⁺ T cell help in the differentiation of rAAV-induced skin T_{RM}. We showed previously that CD4⁺ T cell help was necessary for the optimal generation of long-lived systemic memory T cells following intradermal immunization with rAAV2/1 vectors (34). This also held true in this study for rAAV2/1-induced skin T_{RM}, in line with recent studies in the vaginal mucosa (28) or the lung (26). In some models, CD4⁺ T cell help has been shown to impact CD8⁺ T cell recruitment to the tissue itself (26, 50), although not to vaccinia

virus-infected skin (23). We seldom observed a small reduction in the frequency of CD103⁺ dermal T cells in some experiments, but these results were not systematically reproduced in our hands and their impact was minor compared to the reduction in frequency of OVA₂₅₇⁺ T cells already seen in the blood. Our results suggest that CD4⁺ T cell help directly enhances the level of T cell priming, which impacts the generation of memory precursors from which both T_{CM} and T_{RM} originate (51).

Overall, our results demonstrate the potential of rAAV2/1 vectors to induce bona fide skin T_{RM} and also highlight key elements required for the full differentiation of T_{RM} in this setting. We believe that this study will provide a strong basis to further assess the protective potential of rAAV-induced T_{RM} and the potential use of rAAV vectors in vaccine strategies.

MATERIALS AND METHODS

Mice. Six- to 8-week-old C57BL/6J mice were purchased from JANVIER LABS (Le Genest Saint Isle, France), housed under specific-pathogen-free conditions in our animal facility, and handled in accordance with French and European directives.

Plasmid construction and recombinant AAV vector production. mOVA-HY-expressing constructs and recombinant AAV2/1-pseudotyped vectors were prepared as previously described (38). Briefly, the mOVA cDNA (52) was fused to sequences coding for the DBY₆₀₈ and UTY₂₄₆ epitopes encompassed, respectively, by 5 N-terminal (Nter) and 15 C-terminal (Cter) amino acids, and 4 Nter and 4 Cter amino acids of their original protein sequence to ensure normal processing. This construct was further inserted in a pSMD2 AAV2 plasmid between the human phosphoglycerate kinase (PGK) promoter and a poly(A) signal to create the pSMD2-mOVA-HY construct. For the pSMD2-mOVA-HY-miR construct, 4 repeats of the miR-142-3p target sequence (37) were additionally inserted in the 3' untranslated region of the pSMD2-mOVA-HY plasmid. Two independent lots of both mOVA-HY- and mOVA-HYmiR-expressing rAAV2/1 vectors were used in this study. Optimal titers for immunization (respectively, 3×10^{10} [Fig. 1A to E and 4B, D, and F] and 3×10^9 viral genome [vg] [Fig. 1F, 2, 3, and 4A, C, and E]) were determined for each individual rAAV lot following initial serial dilution experiments, and similar doses were used for both mOVA-HY and mOVA-HYmiR and control rAAV2/1 vectors in a given experiment. For secondary challenge experiments, 3×10^9 vg of an rAAV2/8 expressing a secreted form of OVA was injected. The control vector used throughout this study was an rAAV2/1 vector coding for the Cre recombinase.

Immunizations. For intramuscular or intradermal injection, mice were anesthetized with ketamine/xylazine and 25 μ l of indicated rAAV vector diluted in 1 \times phosphate-buffered saline (PBS) was injected into the tibialis anterior or the ear dermis using a 30-gauge RN Hamilton syringe. For peptide challenges, mice were anesthetized with isoflurane, and OVA₂₅₇ or SMCY₇₃₈ peptides (5 μ g dissolved in 20 μ l of a 4:1 acetone-dimethyl sulfoxide [DMSO] solution) were applied to the dorsal side of the selected ear. The ear skin was then gently poked with a 27-gauge needle around 10 times. Thickness of the ear pinna was measured on anesthetized mice with a digital micrometer (Mitutoyo). For FTY720 treatments, mice received 1 mg/kg of body weight of FTY720 intraperitoneally (i.p.) every 3 days as well as FTY720 in their drinking water (4 μ g/ml) from the day before the secondary challenge until the end of the experiment.

Cell isolation and analysis of cytokine production by T cells. Skin cell suspensions were prepared by separating the ventral and dorsal sheets of immunized ears and incubating them dermal side down in 0.5% trypsin-EDTA (Gibco) for 45 min at 37°C. The epidermis layer was then separated from the dermis layer, and both were cut into small piece and further incubated for 2 h 30 min at 37°C in complete RPMI medium containing 2.5 mg/ml of collagenase D (Roche) and 10 μ g/ml of DNase I (Sigma-Aldrich). The resulting cell suspensions were then filtered on a 40- μ m cell strainer (BD Biosciences) prior to staining. Lymph node cell suspensions were prepared by mechanically dissociating pooled superficial cervical (parotid and mandibular; ear draining) LNs in sterile 1 \times PBS containing 0.1% human serum albumin (HSA). A maximum of 2×10^6 cells per organ were then directly stained or restimulated for 5 h *in vitro* in 2 ml of complete RPMI medium containing 2 μ g/ml of brefeldin A (Sigma-Aldrich) and 1 μ g/ml of OVA₂₅₇ peptide (SIINFEKL; ProteoGenix). For CD107 mobilization assays, monensin (BD GolgiStop; 4 μ l per 6 ml), 0.1 μ g of Alexa Fluor 488 (AF488) anti-CD107a (1D4B), and 0.5 μ g of AF488 anti-CD107b (ABL-93) were also added to each well prior to OVA₂₅₇ peptide stimulation.

Flow cytometry analysis. For peripheral blood lymphocyte (PBL) staining, erythrocytes were first eliminated by hypotonic shock with BD Pharm Lyse buffer (BD Biosciences). Phycoerythrin (PE) H2-K^b/OVA₂₅₇ (SIINFEKL) tetramer (Clinisciences) staining was then performed in 1 \times PBS containing 0.1% HSA for 40 min at room temperature. Cell suspensions were further blocked with anti-CD16/CD32 antibody (2.4G2; BioXcell) for 10 min at 4°C, followed by membrane staining for 15 min at 4°C using a combination of PE, BV605, BV421, or eFluor450 anti-CD8 α (53-6.7), V500 anti-CD4 (RM4-5), fluorescein isothiocyanate (FITC) anti-CD44 (IM7), PE-Cy7 anti-CD62L (MEL-14), PE-Cy7 anti-CD69 (H1-2F3), peridinin chlorophyll protein (PerCP)-Cy5.5 anti-CD45.2 (104), V450 anti-CD45 (30-F1), PerCP-Cy5.5 anti-CD127 (A7R34), allophycocyanin (APC) anti-KLRG1 (2F1/KLRG1), Alexa Fluor 647 anti-CD103 (2E7), APC or biotinylated anti-TCR β (H57-597), PerCP-Cy5.5 anti-Ly6G (1A8), biotinylated anti-Ly6C (AL-21), Alexa Fluor 488 anti-CD11b (M1/70), and Alexa Fluor 770 anti-major histocompatibility complex class II (anti-MHC-II) (I-A/I-E; M5/114.15.2). When necessary, a secondary staining step was performed for 15 min at 4°C with FITC or Qdot 605-coupled streptavidin (Life Technologies). Dead cells were excluded using the LIVE/DEAD Fixable Near-IR dead cell stain kit (Life Technologies). For intracellular staining of cytokines, cells were further

fixed using BD Bioscience Cytofix/Cytoperm buffer (BD Biosciences) according to manufacturer's instructions and subsequent staining was performed in eBioscience permeabilization buffer (eBioscience) for 30 min at 4°C using a combination of PE anti-IL-2 (JES6-5H4), PE-Cy7 anti-TNF- α (MP6-XT22), PE-eFluor610 anti-granzyme B (NGZB), and APC anti-IFN- γ (XMG1.2). Ki-67 staining was performed following cell fixation with the eBioscience Foxp3/transcription factor staining buffer set. Data were collected on a FACSCanto II or LSR-II Fortessa flow cytometer and further analyzed using FlowJo software v9.9.6 (Tree Star).

Statistics. All data are shown as means \pm standard errors of the means (SEM). All statistical analyses were performed using GraphPad Prism Software version 6 (GraphPad, San Diego, CA). Specific tests used for each analysis are indicated in the respective figure legends.

ACKNOWLEDGMENTS

We thank Loredana Saveanu (CRI, Université Paris 7, Paris, France), Nicolas Cuburu (NCI, Bethesda, MD), Aurélie Névéol (LIMSI, Université Paris Saclay, Orsay, France), Jean-Claude Weill, and Claude-Agnès Reynaud (INEM, Université Paris 5, Paris, France) for helpful discussions and Sylvaine You for help with ear thickness measurement.

This work was supported by the Association Française contre les Myopathies (AFM) and Agence Nationale de la Recherche (ANR-11-JSV3 and ANR-15-CE15-0005). A.G. and L.B. were supported by the French Ministry of Research and P.C. by the AFM (postdoctoral fellowship grant no. 18716).

We declare no financial or commercial conflict of interest.

REFERENCES

- Mueller SN, Mackay LK. 2016. Tissue-resident memory T cells: local specialists in immune defence. *Nat Rev Immunol* 16:79–89. <https://doi.org/10.1038/nri.2015.3>.
- Rosato PC, Beura LK, Masopust D. 2017. Tissue resident memory T cells and viral immunity. *Curr Opin Virol* 22:44–50. <https://doi.org/10.1016/j.coviro.2016.11.011>.
- Steinert EM, Schenkel JM, Fraser KA, Beura LK, Manlove LS, Igyártó BZ, Southern PJ, Masopust D. 2015. Quantifying memory CD8 T cells reveals regionalization of immunosurveillance. *Cell* 161:737–749. <https://doi.org/10.1016/j.cell.2015.03.031>.
- Beura LK, Hamilton SE, Bi K, Schenkel JM, Odumade OA, Casey KA, Thompson EA, Fraser KA, Rosato PC, Filali-Mouhim A, Sekaly RP, Jenkins MK, Vezyz V, Haining WN, Jameson SC, Masopust D. 2016. Normalizing the environment recapitulates adult human immune traits in laboratory mice. *Nature* 532:512–516. <https://doi.org/10.1038/nature17655>.
- Thome JJC, Yudanin N, Ohmura Y, Kubota M, Grinshpun B, Sathaliyawala T, Kato T, Lerner H, Shen Y, Farber DL. 2014. Spatial map of human T cell compartmentalization and maintenance over decades of life. *Cell* 159:814–828. <https://doi.org/10.1016/j.cell.2014.10.026>.
- Sathaliyawala T, Kubota M, Yudanin N, Turner D, Camp P, Thome JJC, Bickham KL, Lerner H, Goldstein M, Sykes M, Kato T, Farber DL. 2013. Distribution and compartmentalization of human circulating and tissue-resident memory T cell subsets. *Immunity* 38:187–197. <https://doi.org/10.1016/j.immuni.2012.09.020>.
- Ariotti S, Beltman JB, Chodaczek G, Hoekstra ME, van Beek AE, Gomez-Eerland R, Ritsma L, van Rheenen J, Maree AFM, Zal T, de Boer RJ, Haanen JBAG, Schumacher TN. 2012. Tissue-resident memory CD8+ T cells continuously patrol skin epithelia to quickly recognize local antigen. *Proc Natl Acad Sci U S A* 109:19739–19744. <https://doi.org/10.1073/pnas.1208927109>.
- Ariotti S, Hogenbirk MA, Dijkgraaf FE, Visser LL, Hoekstra ME, Song J-Y, Jacobs H, Haanen JB, Schumacher TN. 2014. T cell memory. Skin-resident memory CD8+ T cells trigger a state of tissue-wide pathogen alert. *Science* 346:101–105. <https://doi.org/10.1126/science.1254803>.
- Schenkel JM, Fraser KA, Beura LK, Pauken KE, Vezyz V, Masopust D. 2014. T cell memory. Resident memory CD8 T cells trigger protective innate and adaptive immune responses. *Science* 346:98–101. <https://doi.org/10.1126/science.1254536>.
- Mackay LK, Rahimpour A, Ma JZ, Collins N, Stock AT, Hafon M-L, Vega-Ramos J, Lauzurica P, Mueller SN, Stefanovic T, Tschärke DC, Heath WR, Inouye M, Carbone FR, Gebhardt T. 2013. The developmental pathway for CD103(+)CD8+ tissue-resident memory T cells of skin. *Nat Immunol* 14:1294–1301. <https://doi.org/10.1038/ni.2744>.
- Skon CN, Lee J-Y, Anderson KG, Masopust D, Hogquist KA, Jameson SC. 2013. Transcriptional downregulation of S1pr1 is required for the establishment of resident memory CD8+ T cells. *Nat Immunol* 14:1285–1293. <https://doi.org/10.1038/ni.2745>.
- Mackay LK, Kallies A. 2017. Transcriptional regulation of tissue-resident lymphocytes. *Trends Immunol* 38:94–103. <https://doi.org/10.1016/j.it.2016.11.004>.
- Mackay LK, Stock AT, Ma JZ, Jones CM, Kent SJ, Mueller SN, Heath WR, Carbone FR, Gebhardt T. 2012. Long-lived epithelial immunity by tissue-resident memory T (TRM) cells in the absence of persisting local antigen presentation. *Proc Natl Acad Sci U S A* 109:7037–7042. <https://doi.org/10.1073/pnas.1202288109>.
- Casey KA, Fraser KA, Schenkel JM, Moran A, Abt MC, Beura LK, Lucas PJ, Artis D, Wherry EJ, Hogquist K, Vezyz V, Masopust D. 2012. Antigen-independent differentiation and maintenance of effector-like resident memory T cells in tissues. *J Immunol* 188:4866–4875. <https://doi.org/10.4049/jimmunol.1200402>.
- Khan TN, Mooster JL, Kilgore AM, Osborn JF, Nolz JC. 2016. Local antigen in nonlymphoid tissue promotes resident memory CD8+ T cell formation during viral infection. *J Exp Med* 213:951–966. <https://doi.org/10.1084/jem.20151855>.
- Muschaweckh A, Buchholz VR, Fellenzer A, Hessel C, König P-A, Tao S, Tao R, Heikenwalder M, Busch DH, Korn T, Kastenmüller W, Drexler I, Gasteiger G. 2016. Antigen-dependent competition shapes the local repertoire of tissue-resident memory CD8+ T cells. *J Exp Med* 213:3075–3086. <https://doi.org/10.1084/jem.20160888>.
- Iborra S, Martínez-López M, Khouili SC, Enamorado M, Cueto FJ, Conde-Garrosa R, del Fresno C, Sancho D. 2016. Optimal generation of tissue-resident but not circulating memory T cells during viral infection requires crosspriming by DNGR-1(+) dendritic cells. *Immunity* 45:847–860. <https://doi.org/10.1016/j.immuni.2016.08.019>.
- Gebhardt T, Wakim LM, Eidsmo L, Reading PC, Heath WR, Carbone FR. 2009. Memory T cells in nonlymphoid tissue that provide enhanced local immunity during infection with herpes simplex virus. *Nat Immunol* 10:524–530. <https://doi.org/10.1038/ni.1718>.
- Ilijima N, Iwasaki A. 2014. T cell memory. A local macrophage chemokine network sustains protective tissue-resident memory CD4 T cells. *Science* 346:93–98. <https://doi.org/10.1126/science.1257530>.
- Masopust D, Choo D, Vezyz V, Wherry EJ, Duraiswamy J, Akondy R, Wang J, Casey KA, Barber DL, Kawamura KS, Fraser KA, Webby RJ, Brinkmann V, Butcher EC, Newell KA, Ahmed R. 2010. Dynamic T cell migration program provides resident memory within intestinal epithelium. *J Exp Med* 207:553–564. <https://doi.org/10.1084/jem.20090858>.
- Thom JT, Weber TC, Walton SM, Torti N, Oxenius A. 2015. The salivary gland acts as a sink for tissue-resident memory CD8(+) T cells, facilitating protection from local cytomegalovirus infection. *Cell Rep* 13:1125–1136. <https://doi.org/10.1016/j.celrep.2015.09.082>.

22. Smith CJ, Caldeira-Dantas S, Turula H, Snyder CM. 2015. Murine CMV infection induces the continuous production of mucosal resident T cells. *Cell Rep* 13:1137–1148. <https://doi.org/10.1016/j.celrep.2015.09.076>.
23. Jiang X, Clark RA, Liu L, Wagers AJ, Fuhlbrigge RC, Kupper TS. 2012. Skin infection generates non-migratory memory CD8⁺ T(RM) cells providing global skin immunity. *Nature* 483:227–231. <https://doi.org/10.1038/nature10851>.
24. Wakim LM, Woodward-Davis A, Bevan MJ. 2010. Memory T cells persisting within the brain after local infection show functional adaptations to their tissue of residence. *Proc Natl Acad Sci U S A* 107:17872–17879. <https://doi.org/10.1073/pnas.1010201107>.
25. Wakim LM, Woodward-Davis A, Liu R, Hu Y, Villadangos J, Smyth G, Bevan MJ. 2012. The molecular signature of tissue resident memory CD8 T cells isolated from the brain. *J Immunol* 189:3462–3471. <https://doi.org/10.4049/jimmunol.1201305>.
26. Laidlaw BJ, Zhang N, Marshall HD, Staron MM, Guan T, Hu Y, Cauley LS, Craft J, Kaech SM. 2014. CD4⁺ T cell help guides formation of CD103⁺ lung-resident memory CD8⁺ T cells during influenza viral infection. *Immunity* 41:633–645. <https://doi.org/10.1016/j.immuni.2014.09.007>.
27. Graham JB, Da Costa A, Lund JM. 2014. Regulatory T cells shape the resident memory T cell response to virus infection in the tissues. *J Immunol* 192:683–690. <https://doi.org/10.4049/jimmunol.1202153>.
28. Cuburu N, Graham BS, Buck CB, Kines RC, Pang Y-YS, Day PM, Lowy DR, Schiller JT. 2012. Intravaginal immunization with HPV vaccines induces tissue-resident CD8⁺ T cell responses. *J Clin Invest* 122:4606–4620. <https://doi.org/10.1172/JCI63287>.
29. Cuburu N, Khan S, Thompson CD, Kim R, Vellinga J, Zahn R, Lowy DR, Schepher G, Schiller JT. 2018. Adenovirus vector-based prime-boost vaccination via heterologous routes induces cervicovaginal CD8⁺ T cell responses against HPV16 oncoproteins. *Int J Cancer* 142:1467–1479. <https://doi.org/10.1002/ijc.31166>.
30. Nieto K, Salvetti A. 2014. AAV vectors vaccines against infectious diseases. *Front Immunol* 5:5. <https://doi.org/10.3389/fimmu.2014.00005>.
31. Jooss K, Yang Y, Fisher KJ, Wilson JM. 1998. Transduction of dendritic cells by DNA viral vectors directs the immune response to transgene products in muscle fibers. *J Virol* 72:4212–4223.
32. Xin K-Q, Mizukami H, Urabe M, Toda Y, Shinoda K, Yoshida A, Oomura K, Kojima Y, Ichino M, Klinman D, Ozawa K, Okuda K. 2006. Induction of robust immune responses against human immunodeficiency virus is supported by the inherent tropism of adeno-associated virus type 5 for dendritic cells. *J Virol* 80:11899–11910. <https://doi.org/10.1128/JVI.00890-06>.
33. Mays LE, Wang L, Lin J, Bell P, Crawford A, Wherry EJ, Wilson JM. 2014. AAV8 induces tolerance in murine muscle as a result of poor APC transduction, T cell exhaustion, and minimal MHC1 upregulation on target cells. *Mol Ther* 22:28–41. <https://doi.org/10.1038/mt.2013.134>.
34. Ghenassia A, Gross D-A, Lorain S, Tros F, Urbain D, Benkhalifa-Ziyyat S, Charbit A, Davoust J, Chappert P. 2017. Intradermal immunization with rAAV1 vector induces robust memory CD8⁺ T cell responses independently of transgene expression in DCs. *Mol Ther* 25:2309–2322. <https://doi.org/10.1016/j.ymthe.2017.06.019>.
35. Pizzolla A, Nguyen TH, Sant S, Jaffar J, Loudovaris T, Mannering SI, Thomas PG, Westall GP, Kedzierska K, Wakim LM. 2018. Influenza-specific lung-resident memory T cells are proliferative and polyfunctional and maintain diverse TCR profiles. *J Clin Invest* 128:721–733. <https://doi.org/10.1172/JCI96957>.
36. Lu Y, Song S. 2009. Distinct immune responses to transgene products from rAAV1 and rAAV8 vectors. *Proc Natl Acad Sci U S A* 106:17158–17162. <https://doi.org/10.1073/pnas.0909520106>.
37. Brown BD, Venneri MA, Zingale A, Sergi Sergi L, Naldini L. 2006. Endogenous microRNA regulation suppresses transgene expression in hematopoietic lineages and enables stable gene transfer. *Nat Med* 12:585–591. <https://doi.org/10.1038/nm1398>.
38. Carpentier M, Lorain S, Chappert P, Laffer M, Harget R, Urbain D, Peccate C, Adriouch S, Garcia L, Davoust J, Gross D-A. 2015. Intrinsic transgene immunogenicity gears CD8⁺ T-cell priming after rAAV-mediated muscle gene transfer. *Mol Ther* 23:697–706. <https://doi.org/10.1038/mt.2014.235>.
39. Zaiss AK, Liu Q, Bowen GP, Wong NCW, Bartlett JS, Muruve DA. 2002. Differential activation of innate immune responses by adenovirus and adeno-associated virus vectors. *J Virol* 76:4580–4590. <https://doi.org/10.1128/JVI.76.9.4580-4590.2002>.
40. Ertl HC. 2016. Viral vectors as vaccine carriers. *Curr Opin Virol* 21:1–8. <https://doi.org/10.1016/j.coviro.2016.06.001>.
41. Grimm D, Zhou S, Nakai H, Thomas CE, Storm TA, Fuess S, Matsushita T, Allen J, Surosky R, Lochrie M, Meuse L, McClelland A, Colosi P, Kay MA. 2003. Preclinical in vivo evaluation of pseudotyped adeno-associated virus vectors for liver gene therapy. *Blood* 102:2412–2419. <https://doi.org/10.1182/blood-2003-02-0495>.
42. Reimsnyder S, Manfredsson FP, Muzyczka N, Mandel RJ. 2007. Time course of transgene expression after intrastriatal pseudotyped rAAV2/1, rAAV2/2, rAAV2/5, and rAAV2/8 transduction in the rat. *Mol Ther* 15:1504–1511. <https://doi.org/10.1038/sj.mt.6300227>.
43. Donahue BA, McArthur JG, Spratt SK, Bohl D, Lagarde C, Sanchez L, Kaspar BA, Sloan BA, Lee YL, Danos O, Snyder RO. 1999. Selective uptake and sustained expression of AAV vectors following subcutaneous delivery. *J Gene Med* 1:31–42.
44. Keswani SG, Balaji S, Le L, Leung A, Lim F-Y, Habli M, Jones HN, Wilson JM, Crombleholme TM. 2012. Pseudotyped adeno-associated viral vector tropism and transduction efficiencies in murine wound healing. *Wound Repair Regen* 20:592–600. <https://doi.org/10.1111/j.1524-475X.2012.00810.x>.
45. Davies B, Prier JE, Jones CM, Gebhardt T, Carbone FR, Mackay LK. 2017. Cutting edge: tissue-resident memory T cells generated by multiple immunizations or localized deposition provide enhanced immunity. *J Immunol* 198:2233–2237. <https://doi.org/10.4049/jimmunol.1601367>.
46. Sallach J, Di Pasquale G, Larcher F, Niehoff N, RübSam M, Huber A, Chiorini J, Almarza D, Eming SA, Ulus H, Nishimura S, Hacker UT, Hallek M, Niessen CM, Büning H. 2014. Tropism-modified AAV vectors overcome barriers to successful cutaneous therapy. *Mol Ther* 22:929–939. <https://doi.org/10.1038/mt.2014.14>.
47. Braun-Falco M, Doenecke A, Smola H, Hallek M. 1999. Efficient gene transfer into human keratinocytes with recombinant adeno-associated virus vectors. *Gene Ther* 6:432–441. <https://doi.org/10.1038/sj.gt.3300815>.
48. Jakobsen M, Askou AL, Stenderup K, Rosada C, Dagnæs-Hansen F, Jensen TG, Corydon TJ, Mikkelsen JG, Aagaard L. 2015. Robust lentiviral gene delivery but limited transduction capacity of commonly used adeno-associated viral serotypes in xenotransplanted human skin. *Hum Gene Ther Methods* 26:123–133. <https://doi.org/10.1089/hgtb.2014.135>.
49. Dang CH, Aubert M, De Silva Feelixge HS, Diem K, Loprieno MA, Roychoudhury P, Stone D, Jerome KR. 2017. In vivo dynamics of AAV-mediated gene delivery to sensory neurons of the trigeminal ganglia. *Sci Rep* 7:927. <https://doi.org/10.1038/s41598-017-01004-y>.
50. Nakanishi Y, Lu B, Gerard C, Iwasaki A. 2009. CD8⁺ T lymphocyte mobilization to virus-infected tissue requires CD4⁺ T-cell help. *Nature* 462:510–513. <https://doi.org/10.1038/nature08511>.
51. Gaide O, Emerson RO, Jiang X, Gulati N, Nizza S, Desmarais C, Robins H, Krueger JG, Clark RA, Kupper TS. 2015. Common clonal origin of central and resident memory T cells following skin immunization. *Nat Med* 21:647–653. <https://doi.org/10.1038/nm.3860>.
52. Calbo S, Delagrèverie H, Arnoult C, Authier F-J, Tron F, Boyer O. 2008. Functional tolerance of CD8⁺ T cells induced by muscle-specific antigen expression. *J Immunol* 181:408–417.
53. Roederer M, Nozzi JL, Nason MC. 2011. SPICE: exploration and analysis of post-cytometric complex multivariate datasets. *Cytometry A* 79:167–174. <https://doi.org/10.1002/cyto.a.21015>.